Why perfusion measurements will fail

Constantin Sandmann, Erik A. Hanson, Alexander Malyshev, Arvid Lundervold, Jan Modersitzki, Erlend Hodneland

Abstract—In perfusion imaging the usage of traditional one-compartment models to estimate hemodynamic parameters like blood flow (perfusion), blood volume and mean transit times is widespread. In this paper we show limits of traditional models to recover perfusion in coupled systems. Based on modeling of porous media flow, we introduce a continuous model for propagation of a tracer in the capillary tissue. We show that the proposed model can be understood as a coupled set of traditional one-compartment models. It is furthermore demonstrated that traditional models (deconvolution, maximum slope) are accurately recovering the perfusion if applied to the full system. However, it is shown both analytically and experimentally that results of traditional models are not meaningful if applied only to smaller portions of the system, and will result in overestimation of perfusion. Evidence of real patient data is provided, indicating that this effect might also be observed in real-life applications. As a remedy, we propose to define perfusion mathematically in coupled systems as laminar flow along the streamlines.

I. INTRODUCTION

Quantitative measurements of hemodynamic medical parameters based on tracer kinetic modeling are widespread both in research and in clinical practice [1]. In the present work, we focus on mathematical models to estimate blood perfusion (cerebral blood flow, CBF), blood volume (cerebral blood volume, CBV), and mean transit time (MTT) of the brain from contrast-enhanced dynamic image data.

While hardware limitations in medical imaging for decades have confined studies to only handle larger tissue regions or full organs, modern imaging technology and voxel based analysis give rise to aspirations about detailed perfusion maps with sub-millimeter precision. Examples of estimated parameter maps are found in i.e. [3], [4]. Quantitative perfusion maps, as well as other parameter maps arising from tracer kinetic modeling, can be combined with anatomical information, and the maps have proven to be of particular value in e.g. stroke studies for localization of trauma. Among the physiological parameters obtainable from tracer kinetic models, CBF has proven to be particularly difficult to reliably describe on a voxel-basis [5]. Causes for these limitations in perfusion estimations are issues in the numerical implementation [5], but might also depend on over-simplified dynamic models, which were originally designed to describe larger volumes of interest [2]. Even though voxel wise perfusion measurements are difficult to establish, examples of perfusion maps are extensively reported in the literature [3], [4].

There have been several approaches to clarify the concept of perfusion in a continuous sense. In [6], dispersion of the arterial input function was simulated using Navier-Stokes equations. It was shown that neglecting to account for dispersion can have adverse impact on perfusion measurements. More recently, a mathematical theory for voxelwise perfusion was introduced in [7] as an alternative to the traditional region of interest (ROI) based models. However, evaluation of the proposed modeling is still pending.

In this work we focus on the validity of traditional perfusion models. We do this by simulating a tissue patch with one inlet, one outlet, and a highly developed capillary system in between. A directional flow field for the patch is set up according to Darcy's law from porous media flow [8], assuming that blood flow is mainly driven by pressure differences. After that, contrast agent propagation in this patch is simulated using standard transport equations. As a result, we show that the resulting 3D system can be equivalently described by a coupled set of multiple traditional one-compartment models, in line with the physical environment where each control volume is feeding the direct neighbors.

We then proceed to demonstrate that traditional models like deconvolution or maximum slope are able to recover the perfusion accurately if applied to the whole system. However, when applying the traditional models to isolated parts of the full system, we find that local perfusion in coupled systems is not straight-forward to define. In order to cope with this issue, two possible definitions of voxel-wise perfusion are presented: A definition P_v which is closely connected to the concept of local arterial input functions and a tailored definition for continuous models P_s.

Our results show that perfusion results from traditional models tend to overestimate P_s and to underestimate P_v if they are applied only to parts of the full system. Analytic results are given, which show that the recovered perfusion depends on all upstream flow and not only on the local value. We also show results indicating that overestimation of perfusion due to coupling might also be found in real data.

In light of expected improvements in spatial resolution of medical scanners, traditional models will increasingly fail to accurately measure blood-flow when applied to patches of the capillary system. Instead, this establishes the need for continuous models as e.g. proposed in [7].

II. TRADITIONAL MODELS FOR PERFUSION

In this section we describe the convolution- and the maximum slope model, two widely used one-compartment pharmacokinetic models for measurements of CBF and CBV. These models were chosen for investigating the behaviour of traditional indicator dilution theory at finer scales. For the remaining, they are referred to as *traditional* models.

Let Ω_i be an arbitrary control volume with one inlet and one outlet, and let $C(t)$ denote the average contrast agent (CA) concentration within Ω_i at timepoint t. The traditional model assumes that the change of concentration at timepoint

t can be described by the ordinary differential equation $C'(t) = P_a c_a(t) - P_v c_v(t)$. Here c_a, c_v are the CA plasma concentrations at the inlet and outlet of Ω_i, and P_a, P_v are the corresponding perfusion values at these locations. Assuming incompressible flow leads to $P_a = P_v$ and hence we obtain the general form

$$C'(t) = P_a \left(c_a(t) - c_v(t) \right). \tag{1}$$

In the following it is assumed that the plasma tracer concentration c_a at the inlet is known. In clinical practice this can be implemented by measuring c_a directly in a feeding artery [10]. Since c_v is usually unknown, additional assumptions need to be made if one wants to reconstruct P_a from a given tissue curve C. The convolution model and the maximum slope (MS) model diverge in further assumptions.

A. The Convolution Model

For the deconvolution model, one approach is to assume there is an unknown probability distribution of transit times h through Ω_i. This leads to

$$c_v(t) = (h * c_a)(t) := \int_0^t c_a(s) h(t - s) \, ds. \tag{2}$$

Combining this with (1) yields $C'(t) = P_a c_a(t) - P_a(h * c_a)(t)$. Integrating this equation and using basic properties of the convolution one obtains the general solution

$$C(t) = (I * c_a)(t). \tag{3}$$

where the *impuls-response function* I is defined as $I(t) := P_a(1 - \int_0^t h(s) \, ds)$. The task of identifying $I(t)$ given a tissue curve $C(t)$ and an arterial input function $c_a(t)$ is a deconvolution problem. If $I(t)$ is recovered, P_a can subsequently be estimated as $P_a = \max_t I(t)$. There are several methods to perform the deconvolution. A standard approach using Fourier-based algorithms is sensitive to the presence of noise [10]. Another class of deconvolution algorithms gaining increasing attention are based on Bayesian modeling [11]. However the numerical handling is still difficult since complex and error-prone numerical integration has to be performed [11]. A popular class among deconvolution algorithms is based on singular value decomposition (SVD) [10]. These algorithms have shown to be robust for a reasonable noise level. Also, they can be easily adapted to be robust against delays in tracer arrival using block-circular structures (bSVD cf. [12]). In order to identify the impuls-response function $I(t)$ from simulated data, we hence decided to use the bSVD model as proposed in [12].

B. The Maximum Slope Model

In the MS model it is assumed that when c_a has its maximum, only a negligible amount of CA is leaving the system [9]. For this time interval, (1) reduces to

$$C'(t) = P_a c_a(t), \tag{4}$$

in case one can see that if c_a has a maximum, also C' must have a maximum since stationarity in P_a is assumed. Hence, it holds that

$$P_a = \frac{\max_t C'(t)}{\max_t c_a(t)}. \tag{5}$$

III. A Synthetic Model for Capillary Flow

The validity of the traditional methods rely on a ROI with only one inlet and one outlet, and that transition times are prescribed by some probability distribution. In fact, the assumption of one inlet and one outlet may easily be violated when we locally describe CA propagation through a larger volume with a highly developed capillary system. For this type of model system we instead expect a set of coupled transport equations where each voxel can be regarded as an inlet for surrounding voxels. Hence, in order to make a realistic synthetic model for capillary flow, we decided to describe the CA propagation as a spatially coupled transport process, i.e. using partial differential equations (PDE) for transport. This PDE model is used for validation of the traditional models.

Compatible with the assumption of stationary, incompressible flow at low Reynold numbers within the capillary system [?], we will use Darcy's law to simulate capillary flow [8]. This is in agreement with previous work on capillary perfusion [?], [?]. A major difference between our coupled flow model and traditional tracer kinetic modeling is the normalization of the flow field within the traditional models, using volume normalized fluid flow with units $[\text{mm}^3/(\text{s}\,\text{mm}^3)]$, referred to as perfusion, as a quantity to describe fluid transport. However, to avoid a discretization dependent flow field, for the PDE model we instead use vector valued surface fluid flux $q = q(x)$ with units $[\text{mm}^3/(\text{s}\,\text{mm}^2)]$, in agreement with geoscience and porous media simulation theory. The fluid flux is a vector field describing the volume of fluid per unit time flowing across a sliced unit area of the sample. Apart from the normalization with respect to surface, the assumptions of linearity and stationarity in the fluid flux are in complete agreement with standard pharmacokinetic modeling [1].

A. Modelling Capillary Blood Flow

For the time being we will not consider contrast agent concentrations, but only the fluid flow in general. The fluid density is denoted by $\rho = \rho(x, t)$. The flux q as well as the porosity are assumed to be stationary and hence independent of time. Fluid entering and leaving the system is described by a source- and sink term $\tilde{Q} = \tilde{Q}(x)$ $[\text{mg}/(\text{s}\,\text{mm}^3)]$. The continuity equation describing conservation of fluid mass states

$$\frac{\partial(\phi\rho)}{\partial t} + \nabla \cdot (\rho q) = \tilde{Q}. \tag{6}$$

Furthermore, assuming that the fluid flow is steady-state and that the density of blood ρ is constant in space, we obtain $\nabla \cdot q = \tilde{Q}/\rho$. In order to scale away the density ρ we define Q $[\text{mm}^3/(\text{s}\,\text{mm}^3)]$ having the relation $\tilde{Q} := Q\rho$, thus transforming the equation into

$$\nabla \cdot q = Q \tag{7}$$

where the right hand side is a volume flux, only non-zero within the source or the sink. Elsewhere, (7) is concurrent with divergence free flow of an incompressible fluid.

Low velocity fluid flux in porous media is usually described by Darcy's law. Neglecting gravitational forces leads to [8]

$$q = -\frac{\mathbf{k}}{\mu} \nabla p. \tag{8}$$

Here, $\mathbf{k} = \mathbf{k}(x)$ is the permeability tensor, $p = p(x)$ is the pressure, and $\mu = \mu(x)$ is the viscosity of the fluid. For simplicity, we will assume that $\mathbf{k}$ is a symmetric and positive definite tensor with only nonzero diagonal elements $\mathbf{k}_{ii} = k$, in accordance with a homogeneous porous medium. Equations (7) and (8) can be combined, yielding the following elliptic partial differential equation in the pressure-field p within the closed domain Ω,

$$\left| \begin{array}{ll} \nabla \cdot \left(-\dfrac{\mathbf{k}}{\mu} \nabla p \right) = Q & x \in \Omega, \\[2mm] n \cdot \nabla p = 0 & x \in \partial\Omega \end{array} \right| \tag{9}$$

where we also added Neuman boundary conditions reflecting zero fluid flux $q(x)$ across $\partial\Omega$. Here, $\partial\Omega$ denotes the boundary of Ω and n the outward unit normal vector. Note that (9) defines a solution which is only unique up to constant [13]. After solving (9) for the pressure p, the flux field can be computed according to (8) from the obtained pressure map.

B. Modelling Indicator Dilution

The introduced framework in Section III-A does not relate flow to propagation of a contrast agent. This section describes a model for CA propagation in the tissue as it is dissolved in the evolving fluid. We assume that the CA is entering the domain along with the fluid flowing in via the source, and similarly extracted at a sink. The resulting CA concentration map is a simulation of the CA concentrations observed within real MRI measurements.

In order to define meaningful and continuous contrast agent concentrations, we first describe the average CA concentration in an (arbitrarily) small tissue volume Ω_i where $C_i(t) := C(x_i, t)$ and $\phi_i := \phi(x_i)$ are assumed to be constant within Ω_i. Assume that V_i is the volume of Ω_i and v_i the the blood volume within Ω_i. By definition, the porosity $\phi_i = v_i / V_i$ reflects the relative space within the vascular system. Let $C_i(t)$ denote the CA concentration in Ω_i with respect to the whole volume V_i at timepoint t. The CA concentration with respect to the blood volume v_i is denoted by $c_i(t)$. From the definition of c_i, C_i and ϕ_i we obtain the relation $C_i(t) = \phi_i c_i(t)$. The rate of change of tracer molecules within an arbitrary control volume Ω_i can he phrased as

$$\frac{\mathrm{d}}{\mathrm{d}t} \int_{\Omega_i} C_i(t)\, \mathrm{d}x = \int_{\Omega_i} \frac{\mathrm{d}}{\mathrm{d}t}(\phi_i c_i(t))\, \mathrm{d}x = \int_{\Omega_i} \phi_i \frac{dc_i}{dt}\, \mathrm{d}x. \tag{10}$$

where the assumption of stationary ϕ_i was used. Since we expect mainly transport and marginal diffusion, the change in tracer mass within Ω_i occurs from advective flow and the source and sink field Q. Let us write the source- and the sink term as $Q = Q_{\mathrm{si}} + Q_{\mathrm{so}}$ where $Q_{\mathrm{si}} < 0$ is the sink and $Q_{\mathrm{so}} > 0$ is the source, and zero elsewhere. Note that $\int_\Omega Q\, \mathrm{d}x = 0$. The change in contrast agent at time point t from fluid entering the control volume can be written as

$$-\int_{\partial\Omega_i} c_i(t)(q_i \cdot n)\, \mathrm{d}s + \int_{\Omega_i} c_a(t) Q_{so,i}\, \mathrm{d}x + \int_{\Omega_i} c_i(t) Q_{si,i}\, \mathrm{d}x, \tag{11}$$

where n is the outward unit normal on $\partial\Omega_i$. In standard pharmacokinetic modeling, c_a is referred to as the arterial

input function (AIF). From the principle of conservation of tracer molecules, equations (10) and (11) must balance for each control volume Ω_i, such that

$$\int_{\Omega_i} \phi_i \frac{dc_i}{dt}\, \mathrm{d}x + \int_{\partial\Omega_i} c_i(t)(q_i \cdot n)\, \mathrm{d}s$$
$$= \int_{\Omega_i} c_a(t) Q_{so,i}\, \mathrm{d}x + \int_{\Omega_i} c_i(t) Q_{si,i}\, \mathrm{d}x. \tag{12}$$

Now, let the contrast agent concentrations, porosity, volume fluxes, and surface flux be continuous functions of space and time. Equation (12) is then consistent with the continuity equation on local form

$$\left| \begin{array}{ll} \phi \dfrac{\partial c}{\partial t} + \nabla \cdot (cq) = c_a Q_{\mathrm{so}} + c Q_{\mathrm{si}} & x \in \Omega,\ t > 0, \\[2mm] c(x,t) = 0 & x \in \Omega,\ t = 0. \end{array} \right| \tag{13}$$

where we also added the initial value $c(x,0) = 0$ in line with the physical problem. Equation (13) is a linear transport equation in $c(x,t)$. Following [13], (13) admits a unique local solution.

C. Relating the transport equation model with the traditional deconvolution model for perfusion

In this section we will describe how the continuous model is related to the traditional deconvolution model. More specifically, we will show that in the continuous model each voxel can be described by a traditional model with arterial input determined by the adjacent upstream voxels.

Let us start by modeling the CA concentration in a given voxel Ω_i using traditional models. For sake of simplicity we assume that $Q_{\mathrm{so},i} = Q_{\mathrm{si},i} = 0$ within that voxel. Note that it is possible to extend the following approach also to voxels where $Q_{\mathrm{so},i} \neq 0$ or $Q_{\mathrm{si},i} \neq 0$. Define the areas (voxel faces) of inflow and outflow over the boundary as $S_{\mathrm{in}} := \{x \in \partial\Omega_i : q_i(x) \cdot n(x) < 0\}$ and $S_{\mathrm{out}} := \{x \in \partial\Omega_i : q_i(x) \cdot n(x) > 0\}$ respectively, following standard notation of positive normal vector n pointing outward. The arterial input Ω_i will be the weighted average of the tracer flux across S_{in}

$$c_{\mathrm{in}}(t) := \frac{\int_{S_{\mathrm{in}}} c(t)(q_i \cdot n)\, \mathrm{d}s}{\int_{S_{\mathrm{in}}} q_i \cdot n\, \mathrm{d}s}. \tag{14}$$

We now define the perfusion within Ω_i as the total fluid inflow divided by the voxel volume,

$$P_{\mathrm{in}} := \frac{-1}{\mathrm{Vol}(\Omega_i)} \int_{S_{\mathrm{in}}} q_i \cdot n\, \mathrm{d}s \tag{15}$$

Given an incompressible flow, Let us now assume that the flow-field q is divergence-free and the amount of CA entering the region is the same as the amount of CA leaving it. Then it holds that $P_{\mathrm{in}} = P_{\mathrm{out}}$ and we can phrase the traditional model as

$$(\phi c_i)'(t) = P_{\mathrm{in}}(c_{\mathrm{in}}(t) - c_{\mathrm{out}}(t)). \tag{16}$$

Note that in the discretization described in Section III-B it is assumed that the CA concentration at the outflow S_{out} equals the concentration within the voxel and that the concentration at the inflow is the concentration at the adjacent voxels. In this case it follows that (16) reduces to the standard equation

for a well-mixed compartment $(\phi c_i)'(t) = P_{\text{in}}(c_{\text{in}}(t) - c_i(t))$ with solution

$$C_i(t) = (I_i * c_{\text{in}})(t) \text{ for } I_i(t) = P_{\text{in}}e^{-P_{\text{in}}/\phi_i t}. \quad (17)$$

The arterial input c_{in} is determined by (14), which recursively depends on all upstream voxels until the global arterial input is reached. To verify this relationship numerically, we simulated a tissue curve $C_i(t)$ using both the continuous PDE model as well as convolution ny (17) with local flow across the voxel faces as the arterial input. We refer to the latter approach as *local convolution*. The two curves have an almost perfect match, as seen in Fig. 1 (left).

As a direct consequence it follows by recursion that for a given voxel at location i the concentration can be written as a convolution of the (global) arterial input function with the impuls-response functions of all upstream voxels $1, \ldots, l$, i.e.

$$C_i(t) = \phi_i((I_1 * \cdots * I_l) * c_{\text{a}})(t). \quad (18)$$

where $I_j(s) := p_i\exp(-p_i(s))$ and $p_i = P_i/\phi_i$. Following [14], the convolution of exponential functions with pairwise different parameters p_i is given by

$$(I_1 * \cdots * I_n)(s) = \sum_{i=1}^{n} \frac{\Pi_{j=1}^{n} p_j}{\Pi_{j=1, j \neq i}^{n}(p_j - p_i)} e^{-p_i s}. \quad (19)$$

See [14] for the case $p_i = p_j$ for some i, j. This relationship was also confirmed experimentally: Figure 1 (right) shows the impulse response function determined by (19) and the impulse response function obtained from deconvolving a tissue curve I_i of the continuous model with the global arterial input function. The two curves coincide almost perfectly.

These results show that the PDE model and the convolution model are equal if the convolution model is applied with the correct, local arterial input. Furthermore, we have shown that the impulse response function obtained by convolution of the global arterial input function is identical to an analytical recursive convolution along all upstream voxels. This clearly demonstrates that the traditional models measure a non-local perfusion quantity along the streamlines, but without accounting for the streamline length when normalizing with respect to volume. Finally, these experiments rule out the error prone deconvolution itself as a major confounding factor in our experiments, since the red and the blue curves in Fig. 1 were almost identical. Thus, the numerical challenges encounted by deconvolution are entirely apart from the challenges encountered by the problem of coupled flow.

D. Converting Flow to Perfusion

The model described in (9) uniquely determines the flux field $q(x)$. However, in pharmacokinetic modeling the parameter of interest is usually the CBF, which we will denote by $P(x)$ as the voxel wise field of perfusion. The surface flux and perfusion are physically distinct, and there are at least two differences between $q(x)$ and $P(x)$. First, the flux is a vector field and the perfusion is a scalar field. Second, the flux is normalized to a surface area and the perfusion is normalized to a volume. Thus, the surface flux and the perfusion are strictly, mathematically different but still conceptually related.
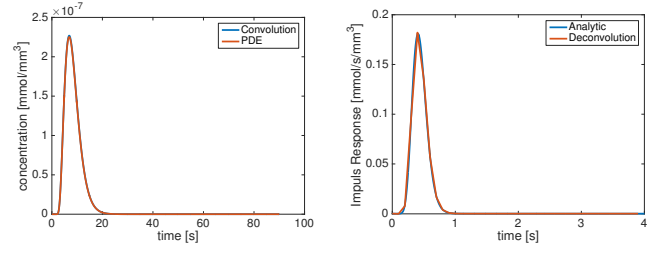

Figure 1. Left: Red curve shows the tissue curve of the continuous PDE model at location [32,35]. Blue curve shows simulation using (17) with $P_i = 5328 \,\text{ml/min/100ml}$ and c_{in} taken locally from upstream voxels around the simulated voxel. The two curves have an almost perfect overlap. Note that the perfusion is unrealisticly high since normalization is performed with respect to the volume of only one voxel. Right: Red curve shows the numerical impulse response functions at location [1,20] using the global arterial input function. Blue curve shows the analytic impulse response function given by (19). The two curves have an almost perfect overlap. These numerical experiments support the analytic considerations, that the computed impulse response function by traditional methods is not the directly feeding impulse response function, but rather a recursive impulse response function depending on all upstream voxels.

In the following we describe a method for converting flux into perfusion, motivated by our need to compare the ground-truth flux field to the scalar valued perfusion field obtained by traditional methods.

The common understanding of perfusion or volume flux $P(x)$ is the amount of blood feeding a tissue volume per unit time, with units $[\text{mm}^3/(\text{s}\,\text{mm}^3)]$. One straightforward approach for converting flux into perfusion could be to estimate the perfusion as the total inflow (or outflow) of fluid (e.g. arterial blood) into a control region per unit time, and then normalizing with the control region volume. This is a valid approach only if the control regions are not feeding each other, and is therefore well-founded for the entire organ. Such understanding of perfusion is in line with the theoretical foundation of traditional compartment models for perfusion where a control region has its own source of feeding arterial blood, independent of neighbor regions.

On the other hand, if the control region is a single voxel or a sub-division of an organ with sequentially feeding arterial blood, the traditional model assumptions are violated since every control region will feed its neighbours, thus becoming a coupled system of flow. Simply summing the total inflow into a voxel and dividing by the voxel volume will strongly over-estimate the perfusion as the normalization refers to the wrong volume. This phenomenon is demonstrated in Fig. 2 where the volume on the left has the true perfusion of $P_1 = F_0/(2V)$ for an incoming flow F_0 $[\text{mm}^3/\text{s}]$ and distribution volume $2V$ $[\text{mm}^3]$. However, for another discretization as shown in the middle, the perfusion within each of these sub-volumes becomes $P_2 = F_0/V = 2P_1$. Taking the average across the two sub-volumes, it is clear that the perfusion is over-estimated with a factor of two. A discretization dependent perfusion estimate is not recommendable, and the perfusion estimate of P_2 is clearly wrong.

In the following we introduce a meaningful notion of perfusion for the continuous model. To do this, we will consider distribution volumes which are following the streamlines. For each point of a streamline we will select a small perpendicular
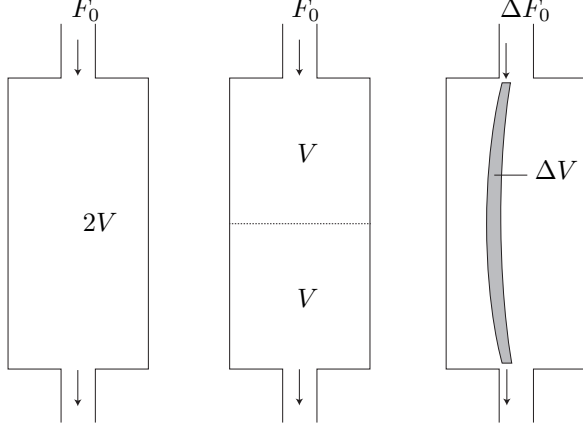
Figure 2. Perfusion within a small volume. Left: A compartment with volume $2V$ is exposed to a flow F_0 [mm^3/s] of fluid. By definition, the perfusion within this compartment becomes $P_1 = F_0/(2V)$. Middle: The same volume is divided into two compartments (e.g. voxels), and the perfusion for each of the compartments becomes $P_2 = F_0/V = 2P_1$. The discrepancy between the two discretizations occurs because the flow is counted twice as it is fed from one voxel to the other. Right: As a solution to the described problem we rather pick out a true distribution volume ΔV (area in this 2D sketch), which is a small area around a given streamline along the centre line of the grey area. This is the true distribution volume (area in this 2D sketch) which is fed with arterial blood from the incoming fractional flow ΔF_0. The correct perfusion within ΔV is therefore $\Delta F_0/\Delta V$. The entire compartment can further be divided into similar infinitesimal distribution volumes, thus providing locally correct perfusion estimates.

disk with radius chosen in such a way that the total flow over each disk is constant along the streamline.

More precisely, let us consider an arbitrary streamline $S \subseteq \Omega \subseteq \mathbb{R}^3$ of length $l > 0$ and parametrization $s : [0, l] \rightarrow \Omega$. We start by calculating the total flow over a small 2-D disk which is perpendicular to the streamline. Let $y \in S$ be an arbitrary location along the streamline. The total flow over a 2-D disk $B_r(y)$ perpendicular to the flow-field $q(y)$ is given by

$$F(y, r) = \int_{B_r(y)} q(x) \cdot \nu \, \mathrm{d}A \text{ where } \nu := q(y)/|q(y)|.$$

In order to calculate the perfusion, we need to establish the volume of a small tube around the streamline. We will not consider a tube with constant radius, but one with spatially varying radii $p : S \rightarrow \mathbb{R}^+$. The total volume of such a tube surrounding the streamline is given by

$$V(p) = \int_0^l \pi(p(s))^2 \, \mathrm{d}s$$

We define the perfusion at an arbitrary point $y \in S$ by

$$P(y) := \lim_{\varepsilon \to 0} \frac{F(y, \varepsilon p(y))}{V(\varepsilon p)} \text{ for } p(x) := 1/\sqrt{|q(x)|}.$$

Note that the radii $p(x)$ are chosen in such a way that in the limit $\varepsilon \to 0$ the total flow is constant along the streamline. To see this, let us assume that q is differentiable with Jacobian J. Using a Taylor expansion of $q(x)$ around y as well as a

change of coordinates yields

$$
\begin{aligned}
F(y, \varepsilon r) &= \int_{B_{\varepsilon r}(y)} \nu^\top q(x) \, \mathrm{d}x \\
&= \int_{B_{\varepsilon r}(y)} \nu^\top q(y) + \nu^\top J(\xi)(x - y) \, \mathrm{d}x \\
&\stackrel{z=(x-y)/(\varepsilon r)}{=} \varepsilon^2 \pi + \int_{B_1(0)} \nu^\top J(\zeta) z (\varepsilon r)^3 \, \mathrm{d}z \\
&= \varepsilon^2 \left(\pi + \varepsilon r^3 \int_{B_1(0)} \nu^\top J(\zeta) z \, \mathrm{d}x \right)
\end{aligned}
$$

for $\xi \in (y, x)$ and $\zeta = (\xi - y)/(\varepsilon r)$.

$$F(y, \varepsilon r) = \varepsilon^2 \left(\pi + \varepsilon \int_{B_1(0)} \nu^\top J(\zeta) \, \mathrm{d}x \right)$$

where $\zeta \in (0, x)$ and simplifications are due to $r = p(y) = 1/\sqrt{|q(y)|}$ and $\nu := q(y)/|q(y)|$. Note that since $V(\varepsilon p) = \varepsilon^2 V(p)$ it follows that

$$P(y) = \frac{\pi}{V(p)} \tag{20}$$

Equation (20) is independent of the spatial location y along the streamline and an explicit formula for converting flux into perfusion, showing that a volume flux like perfusion scales with the distribution volume $V(p)$, which is a function of the streamline length.

E. A Method to Estimate local Porosity

It is known from literature on traditional models for perfusion that CBV for the entire compartment can be expressed as

$$\phi = \frac{\int_0^\infty C(t) dt}{\int_0^\infty c_a(t) dt}. \tag{21}$$

where $C(t)$ are the tracer concentration with respect to a well mixed compartment and $c_a(t)$ is the tracer plasma concentration of the arterial input. However, it is not obvious that (21) is valid also for a continuous one-compartment field model where the voxels are feeding each other. We will now proof that (21) is nevertheless valid.

Returning to the local definition of fluid tracer concentration as $c(x, t)$, the PDE in (13) is consistent with

$$\phi \frac{\partial c}{\partial t} = -q \cdot \nabla c. \tag{22}$$

for locations x where $Q(x) = 0$. Integrating from t_0 to t_1 results in the model

$$\phi[c(x, t_1) - c(x, t_0)] = -\int_{t_0}^{t_1} q \cdot \nabla c \, \mathrm{d}t. \tag{23}$$

Approaching the limit $t_0 = 0, t_1 = \infty$, using the boundary conditions $c(x, 0) = c(x, \infty) = 0$ and defining $E(x) := \int_0^\infty c(x, t) \, \mathrm{d}t$ leads to

$$0 = q \cdot \nabla E(x). \tag{24}$$

We can interpret this equation such that q is tangent to the level-sets of the function $E(x)$, which means that $E(x)$ is constant along the streamlines of the fluid flow. Since at

the beginning of the streamline it holds by construction that $c(x_0, t) = c_a(t)$ and since $C(x, t) = \phi(x)c(x, t)$ it follows that

$$\phi(x) = \frac{\int_0^\infty C(x, t)\, dt}{\int_0^\infty c_a(t)\, dt}. \tag{25}$$

Note that equation (25) coincides with the traditional formula (21) for ϕ.

IV. NUMERICAL EXPERIMENTS

Based on the field models described in Section III, we now establish an experimental setup suited to study the performance of the traditional methods in a synthetic flow field with a known ground truth.

Based on (9) and (13) we set up a forward simulation of blood-flow and indicator dilution through the capillary system. The source can be understood as the arterial space, and the sink can be understood as the venous space. We aimed at creating a transparent synthetic test case and kept all optional parameters as simple as possible.

We chose a standard arterial input function [10], the gamma-variate function

$$c_a(t) := D_0(t - t_0)^\alpha e^{-(t-t_0)/\beta} \tag{26}$$

for default parameters $\alpha = 3$, $D_0 = 1$, $\beta = 1.5\,\mathrm{s}$ and $t_0 = 0\,\mathrm{s}$. Ground truth perfusion for the domain of size $3\,\mathrm{mm} \times 3\,\mathrm{mm} \times 1\,\mathrm{mm}$ was chosen $50\mathrm{ml}/\mathrm{min}/100\mathrm{ml}$. The source term was assigned to the upper left voxel and the sink term was assigned to the lower right voxel. It was assumed that both the domain of inflow as well as outflow were approximately of the voxel-size, leading numerically to Delta-like source and sink terms Q_{so} and Q_{si}. Permeability was chosen isotropic and constant throughout the domain $\mathbf{k} = 5 \times 10^{-6}\,\mathrm{mm}^2$, assuming no directional bias of the capillary system. Dynamic blood viscosity was chosen $\mu = 5 \times 10^{-6}\,\mathrm{kPas}$ according to [15]. Porosity (e.g. CBV) was assumed to be $\phi = 0.05$. Since our aim was to test limits of established methods and to simulate high resolution scans, a voxel size of $(0.05\,\mathrm{mm}, 0.05\,\mathrm{mm}, 3\,\mathrm{mm})$ was assumed. The flow field is visualized in Figure 3 (a).

Equation (9) was solved numerically using two-point flux-approximation (TPFA) widely used in reservoir mechanics [16]. The transport described in (12) was implemented using first order upwinding [17], yielding a 4D CA concentration map $C(x_i, t_j)$. From the porous media model using (9) and (13), streamlines were found from tracking of the flux vector field q by FACT [18], known from tractography within diffusion tensor imaging (DTI).

V. RESULTS

A. Reconstruction of perfusion within synthetic data

We tested the convolution based traditional model (bSVD) (3) as well as maximum-slope (MS) model (5) for their capability to recover perfusion. Prior to reconstruction, the CA concentration map $C(x, t)$ was downsampled to a time-resolution of $0.2\,\mathrm{s}$ in order to stay within comparable time sampling existing on modern MR equipment for dynamic

imaging. In order to simulate different spatial resolutions of the scanning process, the data was averaged using different block-sizes ranging from $(1, 1)$ pixel to $(64, 64)$ pixels. Success of restoration was measured in terms of the relative error of the recovered perfusion with respect to the ground truth perfusion, $RE := |P_{\mathrm{rec}} - P_{\mathrm{true}}/P_{\mathrm{true}} \cdot 100\%$. The recovered perfusion was compared against the two perfusion maps depicted in Figure 3:

The local perfusion map P_{v} was set up using the local definition definition (15). Since normalization is performed with respect to voxel size, the values are unrealistically high and will vary with the discretization. As equation (17) shows, this can nevertheless be regarded a valid definition of perfusion since it models the feeding of arterial blood to a control region. To quantify the errors occurring by traditional methods, the global arterial input function was used for the deconvolution, cf. (19).

The global perfusion map P_{s} was set up using the definition along the streamlines (20). This definition most accurately reflects the physical perfusion at a given location and shows plausible perfusion values, cf. Figure 3. However, we do not expect the traditional models to be able to recover these values accurately.

Results are displayed in Table I. For the complete system, both the maximum slope method and the convolution method could restore the ground truth perfusion of $50\,\mathrm{ml}/\mathrm{min}/100\mathrm{ml}$ accurately with errors of $< 1\%$ and 4% respectively. However, this changes if the methods are applied only to parts of the system. If compared to P_{v}, one can see that results are clearly improving with increasing block size. Note that the block size of $(0.5, 0.5)\mathrm{mm}$ is within the range of resolution available on clinical scanners today, and is therefore clinically interesting. Also a clear advantage of the bSVD method as compared to MS can be observed. This is possibly to the additional assumptions of the MS method. If compared to P_{s}, rendering both methods incapable to recover the physically more meaningful notion of perfusion along the streamlines.

Results from reconstructing ϕ are shown in also shown in Table I, where the relative errors are low for both forward data generated by the transport equation as well as the convolution model. This is supported by the analytic considerations in Section III-E.

Table I
RELATIVE ERROR RE (%) FOR RECONSTRUCTING PERFUSION P_{v}, P_{s} AND THE BLOOD VOLUME ϕ. DISPLAYED IS THE MEDIAN RE. BOTH RECONSTRUCTION MODELS MS AND BSVD ARE ABLE TO RESTORE THE PERFUSION FOR THE ENTIRE DOMAIN, BUT FAIL WHEN DIVIDING THE DOMAIN INTO SMALLER BLOCK SIZES. FOR LARGER BLOCK-SIZES THE BSVD MODEL RESTORES THE PERFUSION MORE ACCURATELY THAN THE MS MODEL. HOWEVER, THE BLOOD VOLUME ϕ IS RECOVERED ACCURATELY. NOTE THAT VOXEL SIZE $(0.05, 0.05)$ CORRESPONDS TO THE ORIGINAL VOXEL SIZE (BLOCK SIZE OF $(1,1)$ VOXELS) IN THE PDE MODEL. FOR A MORE DETAILED DISCUSSION SEE SECTION V-A.

voxel size (mm)	P_{v} bSVD	MS	CBV	P_{s} bSVD	MS
(0.05,0.05)	93%	98%	<1%	423%	95%
(0.23,0.23)	67%	90%	<1%	387%	90%
(0.5,0.5)	44%	79%	<1%	292%	82%
full domain	4%	<1%	<1%		

(a) Flow field   (b) Perfusion P_s along the streamlines   (c) Local perfusion P_v.
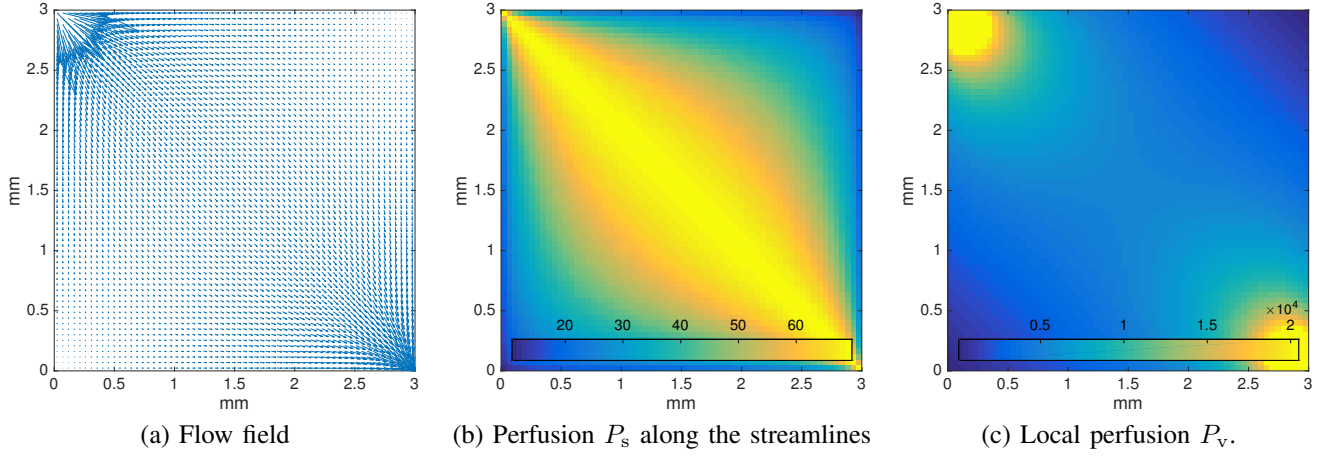
Figure 3. Porous media (PM) flow model with a source in the upper left corner and a sink in the lower right corner. (a) Flow field used to simulate distribution of the contrast agent, (b) Perfusion along the streamlines according to (20), (c) Local perfusion according to (15).

B. Reconstruction of perfusion within real data

Experimental results from Section V-A indicate that application of the deconvolution model to patches of tissues violating the model assumptions would lead to overestimation of blood-flow as compared to the overall flow within the volume of interest. In order to validate this guess, we applied the deconvolution model to a clinically acquired human perfusion CT dataset of a 56 years old male male admitted with suspicion of stroke to the Radboud University Medical Center in Nijmegen, the Netherlands. The perfusion scan was obtained using a Toshiba Aquilon ONE scanner, pixel-size $0.43\,\mathrm{mm} \times 0.43\,\mathrm{mm}$, slice thickness $0.5\,\mathrm{mm}$, contrast agent $50\,\mathrm{mL}$ Xentix 300, total scan-time $114\,\mathrm{s}$, time resolution ranging from $2.1\,\mathrm{s}$ in the early- to $30\,\mathrm{s}$ in the late phase of CA uptake. The arterial input function was manually selected by a medical expert within the middle cerebral artery (MCA). Since we expected to see local overestimation effects mainly for small voxel sizes, the data was processed at full resolution $(512 \times 512 \times 320)$. However, in order to deal with noise effects it was necessary to apply a prior gaussian smoothing with standard deviation of 1 voxel. Relative concentrations were estimated from the CT signal assuming a spatially independent proportionality constant. CBF was then estimated voxel-wise using a Matlab implementation of bSVD, yielding an average CBF of $64.357\,\mathrm{ml/min/100ml}$. After that, we estimated the perfusion for the whole volume of interest by averaging the concentration values first and then performing the bSVD, yielding a total CBF of $24.791\,\mathrm{ml/min/100ml}$. Results are depicted in Fig. V-B

VI. Discussion

In this work we have studied the impact of traditional models to perfusion reconstruction in a coupled system of 1C models. To establish ground-truth values, we developed a PDE based digital phantom to simulate blood flow within a slab of tissue with a highly developed capillary system. We have shown that the discretized PDE problem can be equivalently described as a system of coupled traditional one-compartment models.

The results strongly support the usage of traditional models for entire regions which are fed directly by the measured arterial input. They also show show that if traditional models are applied only to parts of the system, they tend to overestimate the actual perfusion. The reason for this is that traditional models do not take into account the correct distribution volume of the feeding arterial flow. Note that taking local arterial input functions is no remedy for this problem, since the resulting perfusion will depend heavily on the voxel size and overestimate the actual flow, cf. Figure 2 and (17). In fact, in the most extreme example we measured overestimated perfusion values of up to 423%. The results from the digital phantom are supported by real-data experiments, where we showed local overestimation of perfusion for small voxel-sizes as compared to an averaging of concentrations for the entire volume of interest. Regarding the CBV estimates, one can observe from Table I that estimation of blood volume is far more stable, and even various block sizes had little impact on the results. These results are in well agreement with the analytical observations described in Section III-E, stating that (21) is valid for entire organs as well as for single voxels. Thus, these results support the usage of (21) for computing the CBV with high accuracy for any type of block size, including single voxels.

Furthermore we have introduced two conceptually interesting mathematical definitions of voxel perfusion. The global perfusion P_s models perfusion along the streamlines and most accurately models the physical notion of volume flow within the correct distribution volume. Theory and experiments show that the traditional models cannot recover this perfusion. The usage of P_s in reconstructing perfusion might as well be challenging as the entire geometry and microscopical flow patterns would have to be known to track the streamlines. However, for our purpose the understanding of perfusion as a blood flow that must be normalized along its entire length from transition of arterial to venous blood, was useful. On the other hand, for future developments of field models for reconstructing perfusion, multi compartment models as suggested in [7] might be more applicable.

Perfusion P_v was set up based on the interpretation of a

(a) Arterial input function

(b) One slice of the voxel-wise CBF reconstruction.

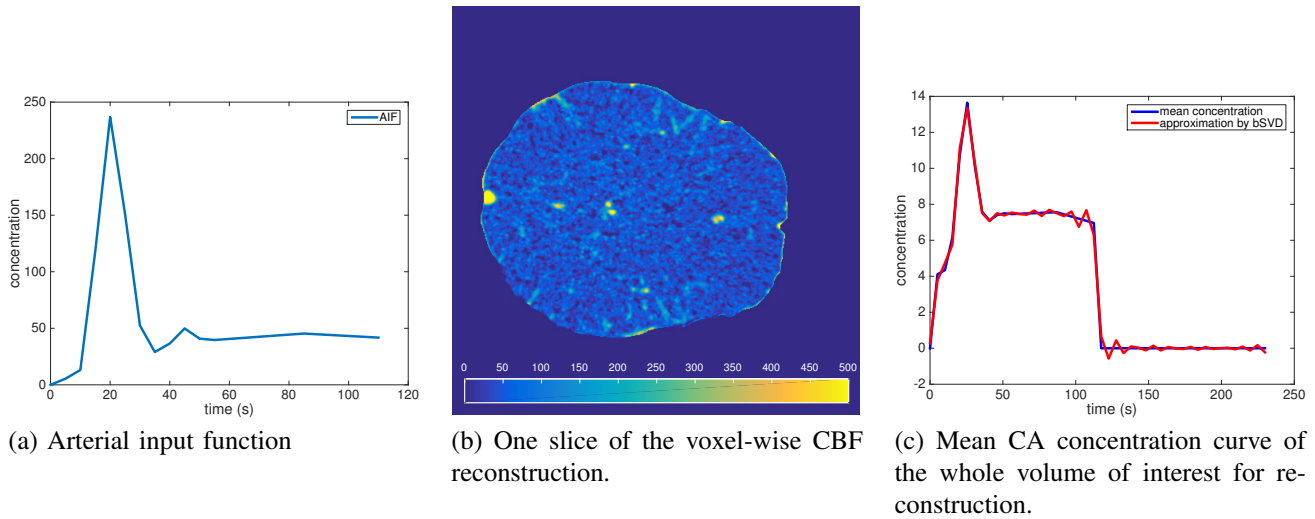(c) Mean CA concentration curve of the whole volume of interest for reconstruction.

Figure 4. Figure with results from the real-data experiments (see Sec. V-B for details on the data). (a) AIF manually selected from the MCA. (b) One slice of the voxel-wise CBF-reconstruction for a 3D volume of interest. (c) Mean concentration curve for the complete 3D volume of interest and the curve approximation by bSVD.

coupled system between adjacent voxels. However, this estimate for perfusion will be over-estimated and was only useful within the computations we performed. Theory and examples show that this definition does not comply with the intended physical notion since it depends heavily on the discretization. However, we have shown that traditional models would restore this value if the correct (local) arterial input function was selected. We have additionally analyzed the impact of selecting a further upstream arterial input function both analytically and experimentally. Specifically we have given an analytic expression which shows that the perfusion will depend on the flow at all upstream voxels, and that the traditional convolution method actually finds the recursive impule response function for all upstream voxels according to (19).

In conclusion, our experiments show that the traditional methods for perfusion estimation perform well when applied to the entire domain, but they tend to fail when applied to smaller block sizes positioned downstream in the flow. The reason for this failure is not numerical instabilities in the deconvolution, but rather over-simplification of a physical phenomenon that is inter-connected in space. The perfusion becomes over estimated as the traditional models will not account for the streamline length of the flow in the transition phase when becoming venous blood, and the same flow will be counted multiple times. This problem is expected to become more pronounced in future as imaging hardware is constantly improving in spatial resolution, yielding high resolution images of sub-millimeter accuracy where a capillary patch with a common arterial input becomes separated between neighboring voxels. To account for this problem, the development of new field models for perfusion is therefore highly demanded, in line with approaches described in [7], [**?**].

REFERENCES

[1] S. Sourbron and D. Buckley, "Classic models for dynamic contrast-enhanced MRI," *NMR Biomed*, vol. 26, no. 8, pp. 1004–1027, 2013.

[2] K. Zierler, "Indicator dilution methods for measuring blood flow, volume, and other properties of biological systems: a brief history and memoir," *Ann Biomed Eng*, vol. 28, no. 8, pp. 836–848, 2000.

[3] Q. Feng *et al.*, "Voxel-level comparison of arterial spin-labeled perfusion magnetic resonance imaging in adolescents with internet gaming addiction," *Behav Brain Funct*, vol. 9, no. 1, p. 33, 2013.

[4] Y. Chen *et al.*, "Voxel-level comparison of arterial spin-labeled perfusion mri and fdg-pet in alzheimer disease," *Neurology*, vol. 77, no. 22, pp. 1977–1985, 2011.

[5] K. Kudo *et al.*, "Differences in CT perfusion maps generated by different commercial software: Quantitative analysis by using identical source data of acute stroke patients 1," *Radiology*, vol. 254, no. 1, pp. 200–209, 2010.

[6] F. Calamante, P. Yim, and J. Cebral, "Estimation of bolus dispersion effects in perfusion MRI using image-based computational fluid dynamics," *Neuroimage*, vol. 19, no. 2, pp. 341–353, 2003.

[7] S. Sourbron, "A tracer-kinetic field theory for medical imaging," *IEEE Trans Med Imaging*, 2014.

[8] H. Darcy, "Les fontaines publiques de la ville de dijon," *Victor Dalmont*, p. 647, 1856.

[9] E. Klotz and M. König, "Perfusion measurements of the brain: using dynamic CT for the quantitative assessment of cerebral ischemia in acute stroke," *Eur J Radiol*, vol. 30, no. 3, pp. 170–184, 1999.

[10] L. Østergaard *et al.*, "High resolution measurement of cerebral blood flow using intravascular tracer bolus passages. part i: Mathematical approach and statistical analysis," *Magn Reson Med*, vol. 36, no. 5, pp. 715–725, 1996.

[11] T. Boutelier *et al.*, "Bayesian hemodynamic parameter estimation by bolus tracking perfusion weighted imaging," *IEEE T Med Imaging*, vol. 31, no. 7, pp. 1381–1395, 2012.

[12] O. Wu *et al.*, "Tracer arrival timing-insensitive technique for estimating flow in mr perfusion-weighted imaging using singular value decomposition with a block-circulant deconvolution matrix," *Magn Reson Med*, vol. 50, no. 1, pp. 164–174, 2003.

[13] L. Evans, *Partial differential equations*, 2nd ed. Providence, Rhode Island: American Mathematical Society, 1998.

[14] W. Kordecki, "Reliability bounds for multistage structures with independent components," *Stat Probabil Lett*, vol. 34, no. 1, pp. 43–51, 1997.

[15] R. Rosencranz and S. Bogen, "Clinical laboratory measurement of serum, plasma, and blood viscosity," *Am J Clin Pathol*, vol. 125 Suppl, pp. 78–86, Jun 2006.

[16] J. Aarnes, T. Gimse, and K.-A. Lie, *An introduction to the numerics of flow in porous media using Matlab*. Springer Verlag, 2007.

[17] S. Patankar, *Numerical Heat Transfer and Fluid Flow*, 1st ed. Hemishpere Publishing Corporation, 1980.

[18] S. Mori, B. Crain, and P. van Zijl, "3D brain fiber reconstruction from diffusion MRI," in *Proceedings of International Conference on Functional Mapping of the Human Brain*, 1998.